

# Stability, effective dimensions, and interactions for bosons in deformed fields

O. Sørensen, D. V. Fedorov, and A. S. Jensen

*Department of Physics and Astronomy, University of Aarhus, DK-8000 Aarhus C, Denmark*

(Dated: March 22, 2002)

The hyperspherical adiabatic method is used to derive stability criteria for Bose-Einstein condensates in deformed external fields. An analytical approximation is obtained. For constant volume the highest stability is found for spherical traps. Analytical approximations to the stability criterion with and without zero point motion are derived. Extreme geometries of the field effectively confine the system to dimensions lower than three. As a function of deformation we compute the dimension to vary continuously between one and three. We derive a dimension-dependent effective radial Hamiltonian and investigate one choice of an effective interaction in the deformed case.

PACS numbers: 05.30.Jp, 03.75.Hh, 31.15.Ja

## I. INTRODUCTION

Bose-Einstein condensation is routinely achieved in a number of laboratories [1, 2, 3, 4], see further descriptions in the recent monographs [5, 6]. The techniques involve cooling and trapping of atomic gases in external laser fields and magnetic fields. These traps are in practice of cylindrical geometry [4, 7, 8]. For  $N$  attractive atoms the stability criterion is experimentally established to be  $N|a_s|/b_t < 0.55$  [8], where  $a_s$  is the scattering length and  $b_t \equiv \sqrt{\hbar/(m\omega)}$  is the relevant length scale of the harmonic trap of geometric average frequency  $\omega \equiv \sqrt[3]{\omega_x\omega_y\omega_z}$ . A reduction from three dimensions to effectively one or two dimensions was observed experimentally [3] in the limit when the interaction energy is small compared to the level spacing in the tightly-confining dimension. Experiments with continuous variation of the trap geometry from three to either one or two effective dimensions [3], with a two-dimensional structure [9, 10], and an effective one-dimensional geometry [11] request a corresponding theoretical description.

Theoretical interpretations and the underlying analyses are frequently based on model assumptions of spherical symmetry [12, 13]. Confinement to lower dimensions can also be studied directly without the three-dimensional starting point [14]. This has been done with a variational calculation in Gross-Pitaevskii equation (GPE) [15] and more recently in the GPE with variational dimensionality [16]. Also effects on stability of deformed external fields have been investigated by use of the GPE formulation [15, 17, 18]. Extreme deformations could result in effective one-dimensional or two-dimensional systems which can be described by effective interactions of corresponding discrete lower dimensions [19, 20, 21, 22].

In the present article we rewrite the hyperspherical formulation from reference [23] to account for a general deformation of the external field. Since two-body correlations are not yet included in the wave function, this hyperspherical approach resembles a mean-field treatment. We investigate the stability criterion in section III. Section IV contains an approach to an effective dimension which depends on the deformation of the external field.

Since the interactions are presently not included in this effective dimension ( $d$ ), we therefore in section V introduce them on top of the derived  $d$ -dimensional Hamiltonian. Although the choice of interactions is not unique, we can with some guess obtain an alternative stability criterion and subsequently interpret the results in terms of a deformation-dependent coupling strength, which is finally compared with known results.

## II. HYPERSPHERICAL DESCRIPTION

A combination of magnetic fields results in an effective trapping potential, which can be described as the deformed harmonic oscillator potential  $V_{\text{trap}}$  acting on all the identical particles of mass  $m$

$$V_{\text{trap}}(\mathbf{r}_i) = \frac{1}{2}m(\omega_x^2 x_i^2 + \omega_y^2 y_i^2 + \omega_z^2 z_i^2), \quad (1)$$

where the position of the  $i$ th particle is  $\vec{r}_i = (x_i, y_i, z_i)$  and the frequencies along the coordinate directions  $q = x, y, z$  are denoted  $\omega_q$ . The hyperradius  $\rho$  is the principal coordinate, which is separated into the components  $\rho_x$ ,  $\rho_y$ , and  $\rho_z$  along the different axes, i.e.

$$\rho^2 = \frac{1}{N} \sum_{i < j}^N r_{ij}^2 = \rho_x^2 + \rho_y^2 + \rho_z^2 \equiv \rho_{\perp}^2 + \rho_z^2, \quad (2)$$

where  $\mathbf{r}_{ij} = \mathbf{r}_j - \mathbf{r}_i$ . In the center-of-mass system the remaining coordinates are given as angles collectively denoted by  $\Omega$ .

An application here of the method presented in reference [23] is to assume a relative wave function as a sum of two-particle components. In the case of a spherical trapping field each two-body component only needs dependence on  $\rho$  and the two-body distance  $r_{ij} = \sqrt{2}\rho \sin \alpha_{ij}$  through an angle  $\alpha_{ij}$ . For a deformed external field it also needs dependence on the angle  $\vartheta_{ij}$  between the interatomic vector  $\mathbf{r}_{ij}$  and the axis of the external field. The two-body component should in the cylindrical case then be on the form  $\phi(\rho, \alpha_{ij}, \vartheta_{ij})$ , which would lead to an angular equation in the two variables  $\alpha_{12}$  and  $\vartheta_{12}$  with

complicated integrals. We shall here restrict ourselves to a wave function which is independent of hyperangles. This is expected to give a fair description for dilute systems where the large distances average out all the directional dependence [24]. This is in contradiction with our conclusions in ref. [25] for repulsive interactions. The mistake was later corrected, see the treatment of attractive interactions in ref. [23].

Thus, we neglect correlations in analogy to a mean-field treatment, so in the dilute limit the hyperangular average of the relative Hamiltonian is

$$\langle \hat{H} \rangle_\Omega \rightarrow \hat{H} = \hat{H}_x + \hat{H}_y + \hat{H}_z + \hat{V}, \quad (3)$$

$$\hat{V} = \sum_{i < j}^N \langle V_{ij} \rangle_\Omega, \quad (4)$$

$$\frac{2m\hat{H}_q}{\hbar^2} = -\frac{1}{\rho_q^{d(N-1)-1}} \frac{\partial}{\partial \rho_q} \rho_q^{d(N-1)-1} \frac{\partial}{\partial \rho_q} + \frac{\rho_q^2}{b_q^4}, \quad (5)$$

where  $d = 1$  and  $b_q^2 \equiv \hbar/(m\omega_q)$  for  $q = x, y, z$ . The interactions  $V_{ij}$  are averaged over all angles  $\Omega$ , which for the zero-range interaction  $4\pi\hbar^2 a_s \delta(\mathbf{r}_{ij})/m$  for  $N \gg 1$  yields

$$\hat{V} = \frac{4\pi\hbar^2 a_s}{m} \sum_{i < j}^N \langle \delta(\mathbf{r}_{ij}) \rangle_\Omega = \frac{\hbar^2}{2m} \frac{1}{2\sqrt{\pi}} N^{7/2} \frac{a_s}{\rho_x \rho_y \rho_z}. \quad (6)$$

If we replace as  $\rho_x = \rho_y = \rho_z = \rho/\sqrt{3}$ , this is identical to the average of the zero-range interaction in the spherically symmetric case [23].

We define the following dimensionless coordinates and parameters:

$$x \equiv \frac{\rho_x}{b_x} \sqrt{\frac{2}{N}}, \quad y \equiv \frac{\rho_y}{b_y} \sqrt{\frac{2}{N}}, \quad z \equiv \frac{\rho_z}{b_z} \sqrt{\frac{2}{N}}, \quad (7)$$

$$\beta \equiv \frac{b_x^2 + b_y^2}{2b_z^2}, \quad \gamma \equiv \frac{b_x^2 - b_y^2}{2b_z^2}, \quad s \equiv \frac{Na_s}{b_t}, \quad (8)$$

$$b_t^3 \equiv b_x b_y b_z. \quad (9)$$

The deformation along the different axes is then described by  $\beta$  and  $\gamma$ , and  $s$  is the effective interaction strength. The Schrödinger equation  $\hat{H}F(\rho_x, \rho_y, \rho_z) = EF(\rho_x, \rho_y, \rho_z)$  is rewritten with the transformation

$$f(x, y, z) \propto (xyz)^{(N-2)/2} F(\rho_x, \rho_y, \rho_z) \quad (10)$$

in order to avoid first derivatives. We then obtain

$$\left[ -\frac{1}{\beta + \gamma} \frac{\partial^2}{\partial x^2} - \frac{1}{\beta - \gamma} \frac{\partial^2}{\partial y^2} - \frac{\partial^2}{\partial z^2} + \frac{N^2 u(x, y, z) - \varepsilon}{2\sqrt{\beta^2 - \gamma^2}} \right] f(x, y, z) = 0, \quad (11)$$

$$u(x, y, z) = \frac{1}{2} \sqrt{\beta^2 - \gamma^2} \left[ \frac{1}{\beta + \gamma} \left( x^2 + \frac{1}{x^2} \right) + \frac{1}{\beta - \gamma} \left( y^2 + \frac{1}{y^2} \right) + z^2 + \frac{1}{z^2} \right] + \sqrt{\frac{2}{\pi}} \frac{s}{xyz}, \quad (12)$$

where  $\varepsilon \equiv 2NE/(\hbar\omega)$ . Without interaction, i.e.  $a_s = 0$ , the ground-state solution is

$$f(x, y, z) = (xyz)^{(N-2)/2} \exp[-N(x^2 + y^2 + z^2)/4], \quad (13)$$

which for  $N \gg 1$  is peaked at  $(x, y, z) = (1, 1, 1)$ .

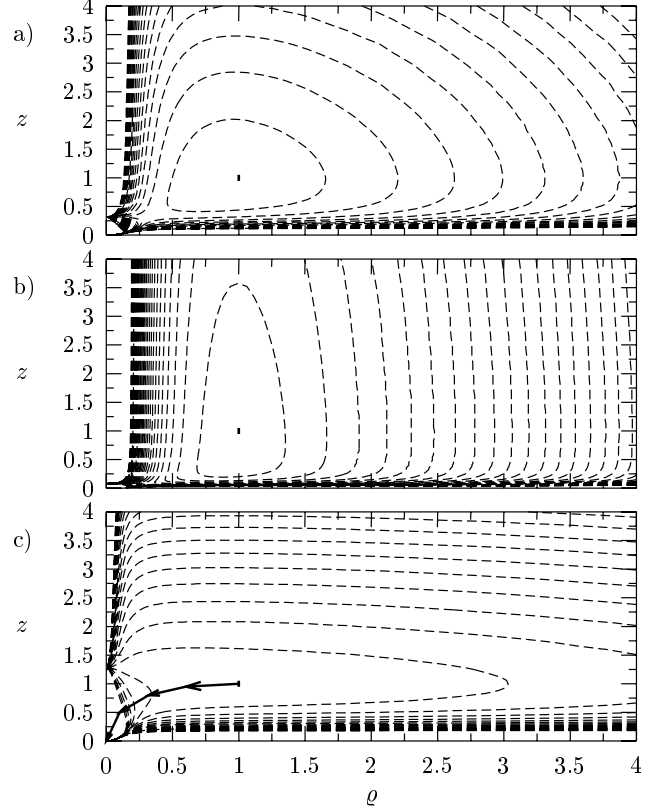


FIG. 1: Contour plots of  $u(x, y, z)$ , eq. (12), with  $x = y = \rho$  as a function of  $(\rho, z)$  for  $s = -0.4\beta^{1/6}$  corresponding to  $Na_s/b_\perp = -0.4$  for three deformations. The values for the contours change by 2, 2, and 5, respectively for a)  $\beta = 1$  (spherical), b)  $\beta = 1/16$  (cigar-shaped or prolate), and c)  $\beta = 16$  (pancake-shape or oblate). In parts a) and b) the minimum at (1,1) is indicated. In part c) the descending path towards (0,0) is indicated.

The wave function in eq. (11) is determined by the properties of the effective potential  $u$ . For axial symmetry around the  $z$  axis the  $x$  and  $y$  directions cannot be distinguished, that is when  $\gamma = 0$  and  $\beta = b_\perp^2/b_z^2$  with  $b_\perp^2 \equiv b_x b_y$ . This symmetry amounts to replacing  $\rho_x^2$  and  $\rho_y^2$  by  $\rho_\perp^2/2$  in the equations. A convenient definition for this case is  $2\rho^2 \equiv x^2 + y^2$ . Equipotential contours of  $u$  in the  $(\rho, z)$  plane for  $\rho = x = y$  are shown in fig. 1 for attractive interactions. For  $a_s < 0$  ( $s < 0$ ) there is always a divergence towards  $-\infty$  when  $(\rho, z) \rightarrow (0, 0)$ , see eq. (12). However, a stationary minimum is seen in both figs. 1a (spherical symmetry) and 1b (prolate) close to  $(\rho, z) = (1, 1)$  (indicated by dots in the figure), whereas this minimum has disappeared for the oblate system in fig. 1c, and no barrier would prevent contraction (indi-

cated by arrows in the figure). For weak attraction a stationary minimum is present for all deformations.

Fig. 2 shows cuts of the potential  $u(\varrho, z)$  along paths close to the bottom of the valleys (see inset). The spherical minimum (full line) is shielded by a relatively small barrier from the divergence for  $\varrho \rightarrow 0$ . The minimum for the prolate deformation (dashed curve) is extremely stable although the divergence for  $\varrho \rightarrow 0$  still exists. For the oblate deformation (dot-dashed line) the local minimum has vanished for this attraction strength.

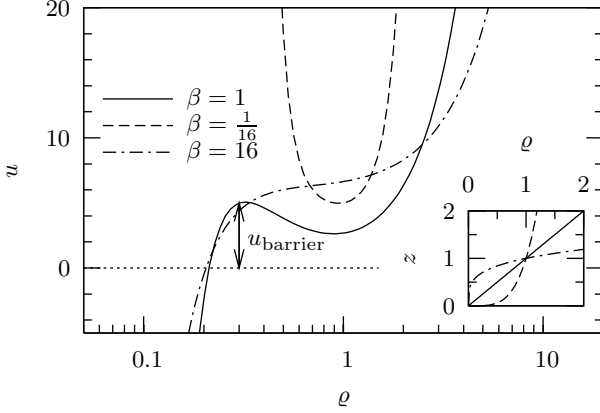


FIG. 2: The potential  $u(x, y, z)$  for  $s = -0.4\beta^{1/6}$  as a function of  $\varrho = x = y$  along cuts of the  $(\varrho, z)$  plane where  $z = \varrho^{1/\sqrt{\beta}}$ . The height  $u_{\text{barrier}}$  of the local maximum at top of the barrier is indicated for the spherical case  $\beta = 1$ . The inset shows corresponding trajectories in the  $(\varrho, z)$  plane, compare with fig. 1, for the three deformations.

### III. STABILITY CRITERION

The barrier height depends on the deformation of the external field, see figs. 1 and 2. Extrema  $(x_0, y_0, z_0)$  of  $u$  in eq. (12) obey the three equations obtained from

$$\frac{b_t^2}{b_x^2}(x_0^4 - 1) = \sqrt{\frac{2}{\pi}} \frac{s x_0}{y_0 z_0} \quad (14)$$

and cyclic permutations of  $x$ ,  $y$ , and  $z$ . This can be used to determine the critical strength  $s$  when the local minimum disappears. The three eqs. (14) can be reduced to find the parameter  $t \equiv 1/z_0^2 - z_0^2$  as a function of  $s$  from the equation

$$s^2 = \frac{\pi}{2} \left( \frac{b_t}{b_z} \right)^4 t^2 \left[ -\frac{1}{2} q_x t + \sqrt{\frac{1}{4} q_x^2 t^2 + 1} \right] \times \quad (15)$$

$$\left[ -\frac{1}{2} q_y t + \sqrt{\frac{1}{4} q_y^2 t^2 + 1} \right] \left[ -\frac{1}{2} t + \sqrt{\frac{1}{4} t^2 + 1} \right], \quad (16)$$

$q_x \equiv \beta + \gamma, \quad q_y \equiv \beta - \gamma.$

The maximum value of the right hand side of eq. (15) is reached when  $t$  is the solution to the equation

$$2 = \frac{q_x t/2}{\sqrt{1 + q_x^2 t^2/4}} + \frac{q_y t/2}{\sqrt{1 + q_y^2 t^2/4}} + \frac{t/2}{\sqrt{1 + t^2/4}}. \quad (17)$$

This solution  $t = t_{\text{max}}$  now from eq. (15) gives the maximum possible value of  $s^2$  when a local minimum of the effective potential  $u$  still is present. Thus we have obtained the largest value of  $s$  where stable solutions exist.

Eqs. (14)-(17) are also obtained for the length parameters  $(b_x, b_y, b_z)$  of a deformed harmonic oscillator ground state wave function by minimizing the expectation value of the GPE mean-field hamiltonian as formulated by Baym and Pethick [15]. This relates the present lowest-order hyperspherical non-correlated results to non-selfconsistent mean-field GPE energies. However, the present results can be improved by including hyperangles in the trial wave function. This enlarges the variational space in ref. [15] and the solutions are improved. The comparison to the self-consistent GPE mean-field results is less direct as the present results are obtained in a different space and especially the hyperangular dependence provides a very different structure for the trial wave function.

The results for axial symmetry ( $\gamma = 0$ ) are shown as the thin solid line in fig. 3. In these units the critical strength  $s$  is largest for a geometry very close to spherical. Since  $s = N a_s / b_t$  and  $b_t^3 = b_x b_y b_z$ , this means that at fixed  $b_t^3$ , or fixed volume, the scattering length can assume the largest negative value for the spherical trap. Gammal *et al.* [17] performed a time-dependent study with the Gross-Pitaevskii equation (GPE) which resulted in the critical strengths here shown as the dotted line. This is in large regions lower than the present result, which might be due to our neglect of the quantum effects of the zero-point energy, which is included later in this paper. The recent value for the experimental stability region [8] is shown as the plus and agrees with the mean-field model. However, the experimental error bars are 10% and almost includes the present result.

These results can be compared to an analytical “spherical” approximation where the radial motion is described by only  $\rho$  while the deformed external field remains the same. The effective radial potential  $U$  is then obtained by adding centrifugal barrier and the contributions from zero-range interaction and the external field. The angular average replaces each of the three components  $\rho_q^2$  and  $R_q^2$  by  $\rho^2/3$  and  $R^2/3$ , where  $\mathbf{R}$  is the center-of-mass coordinates, i.e.

$$\sum_{i=1}^N \langle V_{\text{trap}}(\mathbf{r}_i) \rangle_{\Omega} = \frac{1}{2} m \frac{\omega_x^2 + \omega_y^2 + \omega_z^2}{3} (\rho^2 + N R^2), \quad (18)$$

$$\frac{2m\hat{V}}{\hbar^2} = 8\pi a_s \sum_{i<j}^N \langle \delta(\mathbf{r}_{ij}) \rangle_{\Omega} = \frac{3}{2} \sqrt{\frac{3}{\pi}} N^{7/2} \frac{a_s}{\rho^3}, \quad (19)$$

$$\frac{2mU(\rho)}{\hbar^2} = \frac{3}{2} \sqrt{\frac{3}{\pi}} N^{7/2} \frac{a_s}{\rho^3} + \frac{9N^2}{4\rho^2} + \frac{\rho^2}{l_d^4}, \quad (20)$$

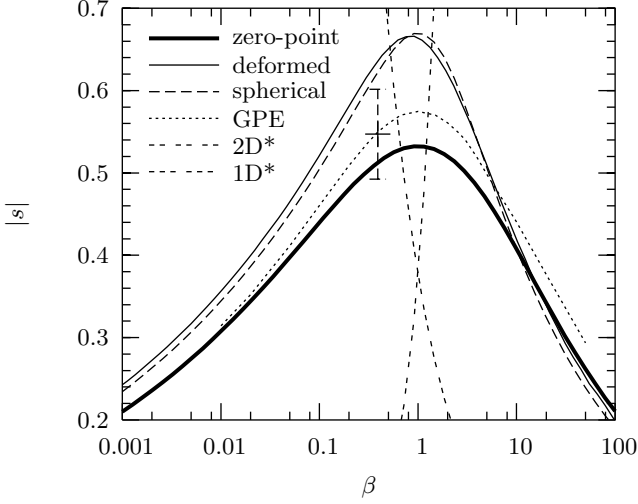


FIG. 3: The critical strength  $|s| = N|a_s|/b_t$  as a function of the deformation  $\beta = b_\perp^2/b_z^2$  from the potential in eq. (12) (thin solid line), from eq. (21) (dashed line), and from a mean-field Gross-Pitaevskii computation by Gammal *et al.* [17] (dotted line). The thick solid line is eq. (23) obtained by considering the zero-point energy. The plus is the experimentally measured value by Claussen *et al.* [8] with the 10% error bars. Regions below curves are considered stable in the separate treatments. The double- and triple-dashed lines indicate the effective cross-overs to two (2D\*) and one (1D\*) dimensions from Görlitz *et al.* [3].

where  $3l_2^{-4} \equiv b_x^{-4} + b_y^{-4} + b_z^{-4}$ . The stability condition becomes

$$\frac{N|a_s|}{b_t} < k(\beta, \gamma), \quad k(1, 0) = \frac{2\sqrt{2\pi}}{5^{5/4}} \simeq 0.67, \quad (21)$$

$$k(\beta, \gamma) = k(1, 0) \sqrt[4]{\frac{3(\beta^2 - \gamma^2)^{4/3}}{2\beta^2 + 2\gamma^2 + (\beta^2 - \gamma^2)^2}}. \quad (22)$$

The spherical limit corresponds to  $\gamma = 0$  and  $\beta = 1$  where the barrier is present when  $|s| = N|a_s|/b_t < 0.67$ . The result for a cylinder (only  $\gamma = 0$ ) is shown as the dashed line in fig. 3 and is noticeably different from, but numerically almost coincides with, the “deformed” treatment, thin solid line. An extreme oblate deformation corresponds to the two-dimensional limit where  $b_z \ll b_\perp$  and  $\beta \rightarrow \infty$ . Here eq. (22) yields the critical strength  $k \simeq 0.4\sqrt[4]{0.6\sqrt{\pi/2}}\beta^{-1/3}$ . As seen from the contour plot in fig. 1c, the motion is now almost confined at  $z = 1$ . From  $x = y = \varrho$  we see that  $u(\varrho, \varrho, 1)$  only has a local minimum when  $|s| < \sqrt{\pi/2}\beta^{-1/3}$ , which is larger than the value where the  $z$  motion is not fixed. This is reasonable since more degrees of freedom in the model lowers the energy. Eq. (15) and Baym and Pethick [15] give the same value in this limit, the latter obtained with a variational study of the GPE provided that the variational width in the axial direction does not change due to the interactions. This is identical to the criterion from studying the potential  $u(\varrho, \varrho, 1)$ , i.e. consistent with the fixed

value  $z = 1$ .

Analogously, in the extreme prolate limit (one-dimensional) where  $\beta \rightarrow 0$ , eq. (22) yields the critical strength  $k \simeq 0.25\sqrt[4]{1.25}\sqrt{\pi}\beta^{1/6}$ . From eq. (15) we obtain in this limit  $k \simeq 3^{-3/4}\sqrt{\pi}\beta^{1/6}$ , which has the same deformation dependence, but is a factor  $\sim 1.7$  larger than the value from eq. (22). However, fixing  $x = y = 1$  in eq. (12) yields no critical strength since  $u(1, 1, z)$  always has a global minimum. Therefore, the other degrees of freedom are essential in this prolate limit.

A better stability criterion can be obtained by considering the ground-state energy  $E_0$  of the boson system, which in the non-interacting case is  $E_0 = \hbar(\omega_x + \omega_y + \omega_z)(N - 1)/2$  where the center-of-mass energy is subtracted. The system is unstable when this energy is larger than the barrier height  $U_{\text{barrier}}$  of the hyperradial potential  $U(\rho)$ ; see the indication in fig. 2 of the corresponding height  $u_{\text{barrier}}$  for the reduced potential  $u$ . With this condition the criterion of stability is

$$\frac{N|a_s|}{b_t} < \frac{1}{2}\sqrt{\frac{\pi}{3}}\frac{l_1}{b_t}\sqrt{1 + \frac{1}{12}\frac{l_1^4}{l_2^4}}, \quad (23)$$

where  $3l_1^{-2} \equiv b_x^{-2} + b_y^{-2} + b_z^{-2}$ . This is seen in fig. 3 (thick solid line) to be below the GPE calculations [17]. The improvement is here substantial compared to when the zero-point energy is neglected. In particular, for the spherical case we get  $N|a_s|/b_t \simeq 0.53$  instead of  $N|a_s|/b_t \simeq 0.67$ . This is within the 10% error bars of the experimental value. The estimate of eq. (23) describes the stability problem better than eqs. (21) and (22) since it includes the quantum effect due to the zero-point energy. An improvement on this would be to solve the hyperradial problem with interaction effects, which would lower the zero-point energy. The critical value would consequently increase, making the present value a lower bound.

A recent variational Monte Carlo investigation of the stability criterion in elongated, almost one-dimensional, traps yielded the stability criterion  $n_{1D}a_{1D} \lesssim 0.35$  [26], where  $n_{1D} \sim N/b_z$  is the density in one dimension and  $a_{1D} = -b_\perp(b_\perp/a_s - 1.0326)$ . Eq. (23) can in the one-dimensional limit be written as  $N|a_s|/b_\perp \lesssim 0.66$ . The deviation between the two results might be due to our use of a three-dimensional zero-range interaction in this non-correlated model, whereas Astrakharchik *et al.* [26] used a one-dimensional model with a zero-range interaction with coupling strength proportional to  $1/a_{1D}$  as well as a full 3D correlated model with hard-sphere or finite-range potentials. An effective potential analogous to  $\delta(x)/a_{1D}$  in the general case with intermediate deformations would be a rewarding goal.

According to Görlitz *et al.* [3] the interaction energy is smaller than the energy in the tightly-confining dimension when  $|s| \leq \sqrt{32/225}\beta^{-5/6}$  for the 1D limit and when  $|s| \leq \sqrt{32/225}\beta^{5/3}$  for the 2D limit. These cross-overs are indicated by double-dashed (two-dimensional) and triple-dashed (one-dimensional) lines in fig. 3. Since the critical region in each limit is below the relevant cross-

over, stable and strongly deformed systems can be regarded as effectively one- or two-dimensional in the sense of these energy relations.

#### IV. EFFECTIVE DIMENSION

The deformation of the external field effectively changes the dimension  $d$  of the space where the particles move. The field changes continuously and  $d$  could correspondingly vary from three to either two or one. In order to arrive at such a description, we aim at an effective  $d$ -dimensional Hamiltonian analogous to eq. (5) with only one radial variable  $\rho$ , a deformation-dependent dimension  $d$ , and an effective trap length  $b_d$ , i.e.

$$\frac{2m\hat{H}_d}{\hbar^2} = -\frac{1}{\rho^{d(N-1)-1}} \frac{\partial}{\partial \rho} \rho^{d(N-1)-1} \frac{\partial}{\partial \rho} + \frac{\rho^2}{b_d^4} + \frac{2m\hat{V}}{\hbar^2}, \quad (24)$$

where  $\hat{V}$  represents all particle interactions in  $d$  dimensions. The requirement is that the Schrödinger equation  $\hat{H}_d G_d = E_d G_d$  with  $d$ -dimensional eigenfunction  $G_d$  and eigenvalue  $E_d$  is obeyed, at least on average, i.e.

$$\int d\rho \rho^{d(N-1)-1} G_d^*(\rho) (\hat{H}_d - E_d) G_d(\rho) = 0. \quad (25)$$

The lowest free solution, that is with  $\hat{V} = 0$ , is given by eq. (13). In the cylindrical case we can relate the  $d$ -dimensional function  $G_d$  to this by performing the average with respect to the angle  $\theta$  in the parametrization  $(\rho_\perp, \rho_z) = \rho(\sin \theta, \cos \theta)$ . With inclusion of the corresponding volume elements this leads to

$$\rho^{d(N-1)-1} |G_d(\rho)|^2 = \rho^{3(N-1)-1} \times \int_0^\pi d\theta \cos^{N-2} \theta \sin^{2N-3} \theta |F(\rho, \theta)|^2, \quad (26)$$

where  $F(\rho, \theta)$  can be obtained by rewriting eqs. (13) and (10).

The characteristic energy and length can be defined by

$$E_d = \frac{d\hbar^2}{2mb_d^2} (N-1), \quad db_d^2 = 2b_\perp^2 + b_z^2, \quad (27)$$

which clearly is correct in the three limits, i.e. spherical:  $d = 3$  and  $b_d = b_z = b_\perp$ , two-dimensional:  $d = 2$  and  $b_\perp \gg b_z$ , and one-dimensional:  $d = 1$  and  $b_z \gg b_\perp$ .

In general it is not possible to find one  $\rho$ -independent set of constants  $(E_d, b_d, d)$  such that  $\hat{H}_d G_d = E_d G_d$ . Instead we insist on the average condition in eq. (25) with  $G_d$  and  $E_d$  from eqs. (26) and (27). The result for axial geometry is a second-degree equation in  $d$  with one physically meaningful root. The results for various  $N$  values are shown in fig. 4. The effective dimension depends on  $N$  for relatively small particle numbers. When  $N > 20$ , the curve is essentially fixed. Furthermore, the asymptotic values of both  $d = 1$  (small  $\beta$ ) and  $d = 2$  (large  $\beta$ ) are reached faster for larger  $N$  since many particles feel

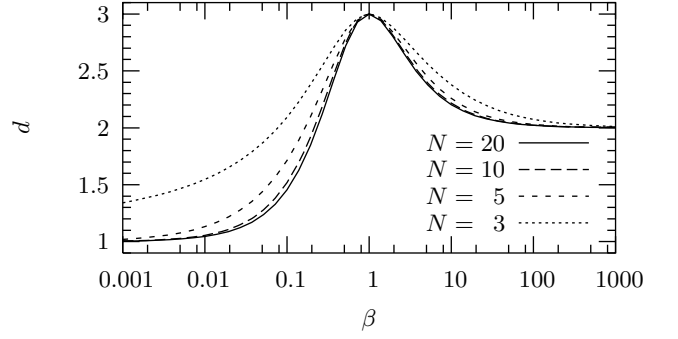


FIG. 4: The effective dimension  $d$  obtained as a function of the deformation parameter  $\beta = b_\perp^2/b_z^2$ . Curves for larger  $N$  are very close to that for  $N = 20$ .

the geometric confinement stronger than few particles. Since these effective dimensions are obtained as average values over  $\rho$ , the system might look spherical at large distances and strongly deformed at small distances, on average resulting in the curves in fig. 4.

#### V. DEFORMATION-DEPENDENT INTERACTIONS

The effective dimension for the non-interacting system possibly changes when interactions are included. The steps of the previous section should in principle be repeated with the interactions. However, this would be complicated and miss the goal which is a simple effective Hamiltonian with a renormalized interaction in lower dimension, see analogies in the references [19, 20, 22].

We therefore start out with a two-body contact interaction with a coupling strength which is modified due to the deformation. This is in line with usual renormalizations due to density-dependent effects [27, 28]; see also a proposed modification due to the inclusion of two-body correlations in the reference [29]. So we write a  $d$ -dimensional zero-range interaction with a dimension-dependent coupling strength  $g(d)$  as

$$V_d(r_{ij}) = g(d) \delta^{(d)}(r_{ij}), \quad g(3) = \frac{\hbar^2 a_s}{m}, \quad (28)$$

where this “ $d$ -dimensional  $\delta$  function” is defined by  $\delta^{(d)}(r) = 0$  for  $r \neq 0$  and  $\int_0^\infty dr r^{d-1} \delta^{(d)}(r) = 1$ . The distance between two particles, e.g. particle 1 and 2, is in hyperspherical coordinates defined by  $r_{12} = \sqrt{2}\rho \sin \alpha$ , where the angle  $\alpha$  enters the angular volume element as

$$d\Omega_\alpha = d\alpha \sin^{d-1} \alpha \cos^{d(N-2)-1} \alpha. \quad (29)$$

This is valid at least for  $d = 1, 2, 3$ . The effective interaction  $\hat{V}$  in eq. (24) is for  $N \gg 1$  then given by the average

over all coordinates except  $\rho$ :

$$\begin{aligned}\hat{V} &= \frac{N^2}{2} \frac{\int_0^{\pi/2} d\Omega_\alpha V_d(\sqrt{2}\rho \sin \alpha)}{\int_0^{\pi/2} d\Omega_\alpha} \\ &= \frac{\hbar^2}{2m} \frac{2N^2(Nd/4)^{d/2}}{\Gamma(d/2)} \frac{a_s g(d)}{\rho^d g(3)}.\end{aligned}\quad (30)$$

However, this does not yield instability for  $d < 2$  since the power  $d$  in  $\rho^{-d}$  is smaller than two.

We therefore pursue another approach. Inspired by the forms of eqs. (19) and (30), we write  $\hat{V}$  as

$$\hat{V} = \frac{\hbar^2}{2m} \frac{2N^2(Nd/4)^{p/2}}{\Gamma(d/2)} \frac{a_d}{\rho^p}, \quad a_3 = a_s, \quad (31)$$

which with  $a_3 = a_s$  coincides with the result for  $d = 3$  if we choose  $p = 3$ . The effective potential  $U_d$  in the  $d$ -dimensional Schrödinger equation corresponding to eq. (24) is then

$$\frac{2mU_d(\rho)}{\hbar^2} = \frac{2N^2(Nd/4)^{p/2}}{\Gamma(d/2)} \frac{a_d}{\rho^p} + \frac{d^2 N^2}{4\rho^2} + \frac{\rho^2}{b_d^4}. \quad (32)$$

For  $p < 2$  this potential always has a global minimum and thus no collapse is present. For  $p > 2$  there is always divergence to  $-\infty$  when  $\rho \rightarrow 0$ . For weak attraction, i.e. small  $|a_d|$ , there is a local minimum. This disappears at larger  $|a_d|$  when

$$\frac{N|a_d|}{b_t} > \frac{b_d^{p-2}}{b_t} \frac{2^{1+p/2} d(p-2)^{(p-2)/4} \Gamma(d/2)}{p(p+2)^{(p+2)/4}}. \quad (33)$$

The criterion in eq. (21) was also obtained by estimating when the critical point vanished. Eq. (21) is valid for all deformations, i.e. any  $d$ . In order to be able to compare eqs. (21) and (33), we therefore choose  $p > 2$  such that eq. (33) always is applicable. When eqs. (33) and (21) agree, the effective interaction strength  $a_d$  is given by

$$\frac{a_d}{a_s} = \frac{b_d^{p-2}}{b_t} \frac{2^{(p-1)/2} \Gamma(\frac{d}{2}) 5^{5/4} (p-2)^{(p-2)/4}}{\sqrt{\pi} (p+2)^{(p+2)/4} \beta^{1/6} p/d} \sqrt[4]{\frac{2+\beta^2}{3}}. \quad (34)$$

This effective interaction strength is in fig. 5 shown as a function of the deformation for various choices of the power  $p$ . The solid line shows the result for  $p = 3$ , which is known to be correct for  $\beta = 1$  ( $d = 3$ ). Similarly the dashed line shows the result with  $p = d$ , which does not work for  $d < 2$  ( $\beta \lesssim 0.2$ ). Since the effective coupling strength depends strongly on the power  $p$ , we need further information about how the interactions enter the effective potential.

An extreme deformation might lead to effectively one-dimensional or two-dimensional properties. Pitaevskii and Stringari [6] collected results for the effective coupling strength in two dimensions that yields  $g(2) = \sqrt{8\pi\hbar^2 a_s/(mb_z)}$ , whereas the result from eq. (34) in that limit is larger by the factor  $5^{5/4}/4 \simeq 1.9$ . Even though

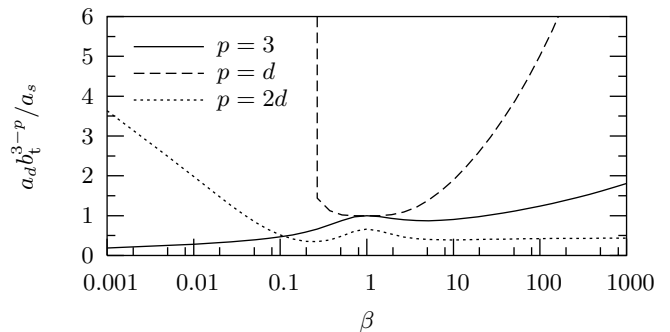


FIG. 5: The effective interaction strength  $a_d$  from eq. (34) obtained as a function of the deformation parameter  $\beta = b_\perp^2/b_z^2$  in the large- $N$  limit, i.e. the connection between deformation and effective dimension obtained from the calculation for  $N = 20$  is used for this illustration. The vertical divergence of the dashed line indicates the inadequacy of the corresponding method when  $d < 2$ .

the results differ by a factor close to two, the right combination of lengths shows that we have incorporated the degrees of freedom in the correct manner. This was also the case in the previous comparison of the stability criterion with the one obtained by Baym and Pethick [15]. However, as was also mentioned by Pitaevskii and Stringari [6], in the low-density limit in two dimensions the coupling constant becomes density-dependent, which is beyond the present model where correlations are neglected.

Since  $p = d$  for  $d = 1$  does not agree with a meaningful interpretation of the stability criterion, a one-dimensional system needs a different treatment.

## VI. DISCUSSION

In conclusion, the hyperspherical method with a non-correlated approach yielded stability criteria as a function of the deformation of the external field. For constant volume the highest stability was found for spherical traps. Effective dimensions  $d$  continuously varying between 1 and 3 were calculated as a function of the deformation. The system can be described by a  $d$ -dimensional effective radial potential with a  $d$ -dimensional effective interaction. However, this does not have an unambiguous form. Applications to restricted geometries become simpler, where the obtained two-dimensional coupling strength compares reasonably with a coupling strength obtained by an axial average of a three-dimensional contact interaction. For the one-dimensional case an effective coupling strength was not obtained.

A previous approach to a  $d = 1$  treatment by Gammal *et al.* [30] shows that a three-body contact interaction is necessary for the GPE to produce collapse in one spatial dimension. In the present framework a three-body contact interaction for a constant angular wave function produces a hyperradial potential proportional to  $\rho^{-2d}$  which

for any  $d \geq 1$  leads to instability if the three-body coupling strength is sufficiently negative. The dotted line in fig. 5 shows the effective coupling strength for  $p = 2d$ , corresponding to this three-body zero-range interaction.

According to Astrakharchik *et al.* [26, 31] a Jastrow ansatz for a correlated wave function and inclusion of two-body interactions lead to collapse in one spatial di-

mension. According to Faddeev calculations with the two-body correlated model presented in reference [23], a two-body interaction and inclusion of only two-body correlations in one spatial dimension do not lead to collapse. It seems that at least three-body correlations or three-body interactions are necessary in order to achieve a realistic description of collapse in one dimension.

- 
- [1] C. A. Sackett, J. M. Gerton, M. Welling, and R. G. Hulet, *Phys. Rev. Lett.* **82**, 876 (1999).
  - [2] J. Stenger *et al.*, *Phys. Rev. Lett.* **82**, 2422 (1999).
  - [3] A. Görlitz *et al.*, *Phys. Rev. Lett.* **87**, 130402 (2001).
  - [4] J. L. Roberts *et al.*, *Phys. Rev. Lett.* **86**, 4211 (2001).
  - [5] C. J. Pethick and H. Smith, *Bose-Einstein Condensation in Dilute Gases* (Cambridge University Press, Cambridge, 2002).
  - [6] L. P. Pitaevskii and S. Stringari, *Bose-Einstein Condensation* (Clarendon Press, Oxford, 2003).
  - [7] E. A. Donley *et al.*, *Nature (London)* **412**, 295 (2001).
  - [8] N. R. Claussen *et al.*, *Phys. Rev. A* **67**, 060701 (2003).
  - [9] M. Greiner *et al.*, *Phys. Rev. Lett.* **87**, 160405 (2001).
  - [10] D. Rychtarik, B. Engeser, H.-C. Nägerl, and R. Grimm, E-print arXiv cond-mat/0309536 (2003).
  - [11] B. L. Tolra *et al.*, E-print arXiv cond-mat/0312003 (2003).
  - [12] J. L. Bohn, B. D. Esry, and C. H. Greene, *Phys. Rev. A* **58**, 584 (1998).
  - [13] S. K. Adhikari, *Phys. Rev. A* **66**, 013611 (2002).
  - [14] Y. E. Kim and A. L. Zubarev, *J. Phys. B: At. Mol. Opt. Phys.* **33**, 55 (2000).
  - [15] G. Baym and C. J. Pethick, *Phys. Rev. Lett.* **76**, 6 (1996).
  - [16] B. A. McKinney and D. K. Watson, *Phys. Rev. A* **65**, 033604 (2002).
  - [17] A. Gammal, T. Frederico, and L. Tomio, *Phys. Rev. A* **64**, 055602 (2001).
  - [18] S. K. Adhikari, *Phys. Rev. E* **65**, 016703 (2002).
  - [19] M. Olshanii, *Phys. Rev. Lett.* **81**, 938 (1998).
  - [20] D. S. Petrov, M. Holzmann, and G. V. Shlyapnikov, *Phys. Rev. Lett.* **84**, 2551 (2000).
  - [21] D. S. Petrov and G. V. Shlyapnikov, *Phys. Rev. A* **64**, 012706 (2001).
  - [22] M. D. Lee, S. A. Morgan, M. J. Davis, and K. Burnett, *Phys. Rev. A* **65**, 043617 (2002).
  - [23] O. Sørensen, D. V. Fedorov, and A. S. Jensen, *Phys. Rev. A* **66**, 032507 (2002).
  - [24] O. Sørensen, D. V. Fedorov, and A. S. Jensen, *J. Phys. B: At. Mol. Opt. Phys.* **37**, 93 (2004).
  - [25] O. Sørensen, D. V. Fedorov, A. S. Jensen, and E. Nielsen, *Phys. Rev. A* **65**, 051601(R) (2002).
  - [26] G. E. Astrakharchik, D. Blume, S. Giorgini, and B. E. Granger, *Phys. Rev. Lett.* **92**, 030402 (2003).
  - [27] T. D. Lee, K. Huang, and C. N. Yang, *Phys. Rev.* **106**, 1135 (1957).
  - [28] E. Braaten, H.-W. Hammer, and T. Mehen, *Phys. Rev. Lett.* **88**, 40401 (2002).
  - [29] O. Sørensen, Ph.D. thesis, Department of Physics and Astronomy, University of Aarhus, Denmark; E-print arXiv cond-mat/0401323, 2004.
  - [30] A. Gammal, T. Frederico, L. Tomio, and F. K. Abdullaev, *Phys. Lett. A* **267**, 305 (2000).
  - [31] G. E. Astrakharchik, D. Blume, S. Giorgini, and B. E. Granger, E-print arXiv cond-mat/0310749 (2003).